PHYSICS AND CHEMISTRY OF SOLID STATE
V. 23, No. 3 (2022) pp. 531-535
Section: Physics

DOI: 10.15330/pcss.23.3.531-535

Vasyl Stefanyk Precarpathian National University

ФІЗИКА І ХІМІЯ ТВЕРДОГО ТІЛА
Т. 23, № 3 (2022) С. 531-535
Фізико-математичні науки

PACS 68.37.Lp, 73.50.–h, 73.61.–r, 81.15.Ef ISSN 1729-4428

A.M. Lohvynov, I.V. Cheshko, I.M. Pazukha, K.V. Tyschenko,
O.V. Pylypenko, A.Yu. Zahorulko

Effect of Ru Interlayer thickness on Electrophysical Properties of Co/Ru/Co three-layer film systems

Sumy State University, Sumy, Ukraine, a.logvinov@aph.sumdu.edu.ua

In this paper, the investigation of the crystal structure and electrophysical properties of Co/Ru/Co/Sub three-layer film systems with a Ru layer thickness d_{Ru} = 5-20 nm has been carried out. It is shown that for both as-deposited and annealed at 800 K thin-film samples the phase composition corresponds to hcp-Co + hcp-Ru. The dependence of resistivity and temperature coefficient of resistance as a function of d_{Ru} was received. It was demonstrated that the change in the resistivity value during the first cycle of heat treatment stays more significant than more Ru layer thickness. The value of temperature coefficient of resistance has an order of 10^{-4} and growth from $5.05 \cdot 10^{-4}$ to $6.42 \cdot 10^{-4}$ K^{-1} within the d_{Ru} range 0-20 nm.

Keywords: three-layer film systems, layer-by-layer condensation, electrophysical properties, resistivity, temperature coefficient of resistance

Received 31.01.2022; Accepted 26.07.2022

Introduction

Nowadays, a lot of different types of spin-valve structures (SVs) were created [1-3]. Such structures are promising for application as functional elements of electronic devices [4-7]. One of the necessary conditions at the formation of SVs is the stability of magnetic and non-magnetic layers. Traditional application of Cu [8], Ag [9], or Au [10] as a non-magnetic layer for separation magnetic layers (Co, Fe, Ni, or their alloys) has some problems. These are intensive diffusion between layers, destruction of interfaces, and solid solution formation. As a result, magnetic layers lose the ability to focus magnetization and the structure ceases to function as a spin-valve [8, 10-12]. The solution to this problem may be the use of additional thin buffer layers between the working layers [13, 14]. Also, reliable separation of the Co or NiFeCuMo layer can be achieved through the use of Ru layers with an effective thickness of 0.2 to 3 nm [15, 16]. Besides, thin-film systems based on Co and Ru have stable magnetic properties and can be used as a synthetical antiferromagnetic layer in the spin-valve structures [17].

Resistivity is one of the base parameters which affect the electronic, strain, magnetic, etc. properties of thin-film systems [18-21]. So, the resistivity (conductivity) of thin-film materials with a polycrystalline structure is widely analyses theoretically and experimentally [22-24].

In this paper, we investigated electrophysical properties of Co/Ru/Co/Sub three-layer film systems with the purpose to establish a general trend of the influence of Ru layer thickness on the resistivity and temperature coefficient of resistance of the tree-layer system. It allows selecting a more thermally stable system for SVs formation.

I. Experimental Procedure

Co thin-film with a thickness d = 40 nm and Co(20)/Ru(d_{Ru})/Co(20)/Sub three-layer film systems with the thickness of Ru in the range of d = 5-20 nm were sputtered by electron-beam evaporation on the glass-ceramic substrate at room temperature. The base chamber pressure was 10^{-4} Pa. The deposition rate was 1.0 nm/s. At such condensation conditions, all samples have nanocrystalline structure and do not contain impurities

phases like oxides or carbides [25, 26].

For stabilization electrophysical properties, the investigated samples were annealed during two cycles "heating ↔ cooling" up to the annealing temperature (T_{ann}) of 800 K. The annealing was performed in a vacuum chamber at 10^{-4} Pa. The measurement of resistivity is carried out in current in plane geometry. The value of temperature coefficient of resistance (TCR) has been calculated on the base of temperature dependences of resistivity by the equation: $\beta = (1/\rho_{in})\cdot(\Delta\rho/\Delta T)$, where ρ_{in} is the initial value of resistivity, ΔT = 5 K.

Crystalline structures of the samples were investigated by transmission electron microscopy (TEM-125K).

II. Results and discussion

The detail analysis of crystal structure of thin-film systems based on Co and Ru and pure Ru thin films were performed in Ref. [25, 26]. It was demonstrated that the diffraction patterns from Co/Ru/Co/Sub three-layer film systems in as-deposited state consist of a combination of a two hexagonal close-packed (hcp) crystal structures with lattice constants a = 0.270 nm, c = 0.429 nm (hcp-Ru), and a = 0.251 nm, c = 0.407 nm (hcp-Co). The following annealing process appears to crystallization of the Ru and Co layers, diffraction rings become sharper, and meanwhile the phase state of the total system doesn't change (Fig. 1(a)).

Figures 1(b)–(c) show the alteration of crystal structures of the Co(20)/Ru(10)/Co(20)/Sub three-layer thin-film system during annealing up to 800 K. For samples Co(20)/Ru(10)/Co(20)/Sub in as-deposited state, the average grain size is ranged from 5 to 7 nm (Fig. 1(b)). After annealing the average grain size grows to 28-30 nm.

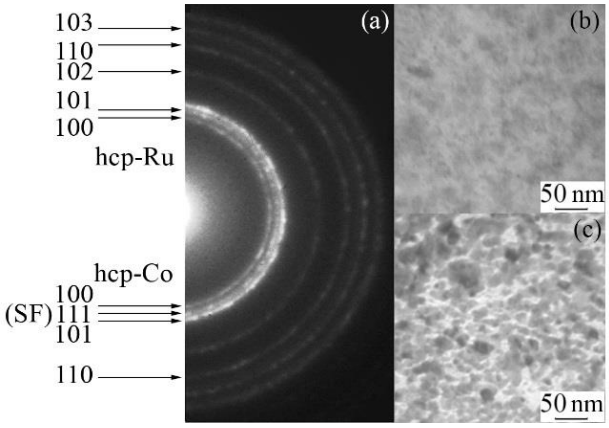

Fig. 1. Diffractions pattern (a) and bright-field TEM images for Co(20)/Ru(10)/Co(20)/Sub three-layer thin-film system after deposition (b) and heat treatment at 800 K (a, c) (SF is stacking fault).

At the electrophysical properties investigation of three-layer film systems, additional research of pure Co(40)/Sub was done. It allows to analyses how the change of the Ru interlayer affects the resistivity and TCR of investigated systems. The results of these investigations are presented in Fig. 2. Note the general peculiarities of the temperature of resistivity. At the stabilization process, the irreversible change of resistivity of the pure Co thin-

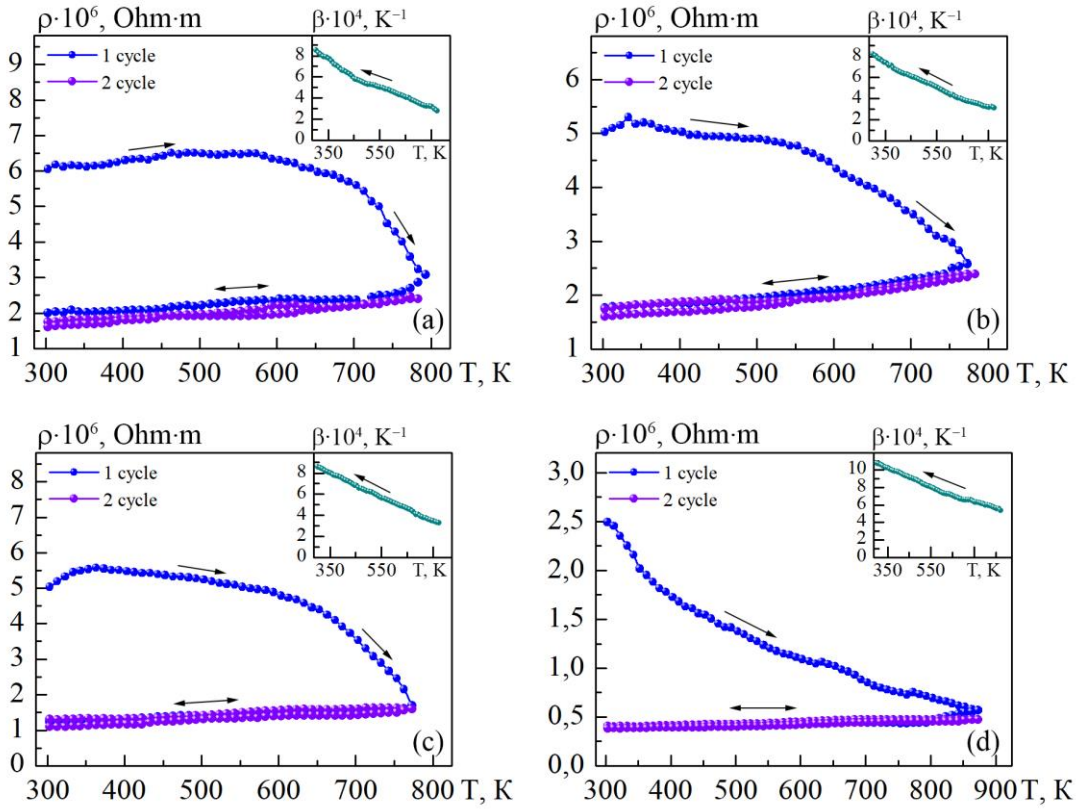

Fig. 2. Temperature dependences of resistitivity and temperature coefficient of resistance (in the insert) for Co(40)/Sub thin-film (a) and Co(20)/Ru(d_{Ru})/Co/Sub three-layer film systems at the thickness of Ru interlayer d_{Ru} = 5 nm (b), 10 nm (c) and 20 nm (d).

Table 1

Experimental and calculation data of TCR for Co/Ru/Co three-layer thin-film systems.

Sample	Co(20)/Ru(5)/Co(20)	Co(20)/Ru(10)/Co(20)	Co(20)/Ru(20)/Co(20)
$\beta_{exp}\cdot 10^3$, K^{-1}	5.20	5.48	6.42
$\beta_{calc}\cdot 10^3$, K^{-1}	5.09	5.34	6.18
$\Delta\beta = (\beta_{exp} - \beta_{calc})\cdot 10^3$, K^{-1}	0.11	0.14	0.24
$\frac{\beta_{\exp} - \beta_{calc}}{\beta_{\exp}}$, %	2.11	2.55	3.74

film and Co/Ru/Co/Sub film systems is observed. It is a result of healing defects and recrystallization processes. At the second cycle of heat treatment, the typical for the metal thin film temperature dependence of resistivity is observed [23, 25]. Namely, the value of resistivity grows at the increase of temperature by the linear low. Besides, the change in the resistivity value during the first cycle of heat treatment stays more significant than more d_{Ru}. The resulting dependence $\rho(d_{Ru})$ is presented in Fig. 3(a). So, the adding of Ru interlayer with a thickness of 5 nm leads to an insignificant decrease of resistivity value. At the same time, the following increase of Ru interlayer thickness up to 20 nm causes the fall of ρ in order.

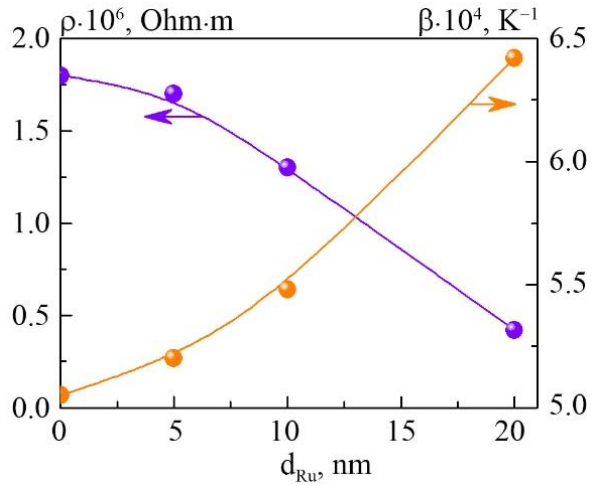

Fig. 3. The resistivity (a) and temperature coefficient of resistance (b) as a function of the Ru interlayer thickness for Co(20)/Ru(d_{Ru})/Co/Sub at d_{Ru} = 0-20 nm.

The temperature dependences of TCR are presented in the insert of Fig. 2. It is evidence the decrease of β value during annealing for all investigated samples. It is fully in agreement with the TCR concept. The value of $\beta \sim 1/\rho$. Note, the value of temperature coefficient of resistance has an order of 10^{-4} and growth from $5.05\cdot 10^{-4}$ to $6.42\cdot 10^{-4}$ K^{-1} within the d_{Ru} range 0-20 nm (Fig. 3(b)).

From a practical point of view, it is advisable to implement a procedure for predicting the electrophysical properties of thin-film systems. Investigations of phase state and diffusion profiles of Co/Ru/Sub and Ru/Co/Sub systems presented in Ref. [25] showed that before and after annealing, the individuality of the layers remains. So, for the prediction of TCR value, the macroscopic model [27] was used. The peculiarity of this model is next. It does not take into account the influence of the microscopic parameters, like the mean free path, mean grain size. In the frame of the macroscopic model, the main equation for TCR can be written in the form:

$$\beta = \beta_1 + \beta_2 + \beta_3 - \frac{d_1\rho_2\rho_3(\beta_2+\beta_3)}{d_1\rho_2\rho_3 + d_2\rho_1\rho_3 + d_3\rho_1\rho_2} - \frac{d_2\rho_1\rho_3(\beta_1+\beta_3) + d_3\rho_1\rho_2(\beta_1+\beta_2)}{d_1\rho_2\rho_3 + d_2\rho_1\rho_3 + d_3\rho_1\rho_2},$$

where β_i, ρ_i and d_i are the TCR, resistivity and thickness for i-layer.

The calculation results presented in Table 1.

The analysis of experimental and calculation data confirm that the macroscopic model satisfactorily describes the experimental results and can be used for the prediction of TCR value for Co/Ru/Co/Sub three-layer film systems. A certain difference in the obtained data can be explained by the insignificant diffusion processes at the interfaces. It causes the change in interface scattering of charge carriers. One more reason is the influence of thermal macro stresses.

Conclusions

The metallic behavior of temperature dependence of resistivity with a positive TCR value was observed for Co(20)/Ru(d_{Ru})/Co/Sub three-layer film systems regardless of the Ru layer thickness. The increasing of Ru interlayer thickness from 5 to 20 nm leads to a fall in order. At the same time, the TCR value has an order of 10^{-4} and grows from $5.05\cdot 10^{-4}$ to $6.42\cdot 10^{-4}$ K^{-1} at the d_{Ru} increase. The analysis of experimental and calculation data in the frame of the macroscopic model confirms that this model can be used for the TCR values prediction.

Acknowledgement

This work was funded by the State Program of the Ministry of Education and Science of Ukraine 0120U102005.

Lohvynov A.M. (corresponding author) – Ph.D (Physics and Mathematics), Engineer of the Electronics, General and Applied Physics Department
Cheshko I.V. – Ph.D (Physics and Mathematics), Associated Professor of the Electronics, General and Applied Physics Department
Pazukha I.M. **–** Ph.D (Physics and Mathematics), Associated Professor of the Electronics, General and Applied Physics Department;
Tyschenko K.V. – Ph.D (Physics and Mathematics), Senior Lecture of the Electronics, General and Applied Physics Department
Pylypenko O.V. – Ph.D (Physics and Mathematics), Senior Lecture of the Electronics, General and Applied Physics Department
Zahorulko A.Yu. – student of the Electronics, General and Applied Physics Department.

[1] W. Zhao, C. Liu, W. Huang, C. Hou, Z. Chen, Z. L-Y. Yin. Positive and negative magnetoresistances in Co/Cu/Ni spin-valves, Mater. Lett. 240, 124-127 (2019); https://doi.org/10.1016/j.matlet.2018.12.134.
[2] M.Z. Iqbal, G. Hussain, S. Siddique, M.W. Iqbal, Graphene spin valve: An angle sensor, J. Magn. Magn. Mater. 432, 135-139 (2017);http://dx.doi.org/10.1016/j.jmmm.2017.02.004.
[3] K. Zhao, Y. Xing, J. Han, J. Feng, W. Shi, B. Zhang, Z. Zeng. Magnetic transport property of NiFe/WSe_2/NiFe spin valve structure, J. Magn. Magn. Mater. 432, 10-13 (2017); http://dx.doi.org/10.1016/j.jmmm.2017.01.066.
[4] H. Piskin, N. Akdogan. Interface-induced enhancement of sensitivity in NiFe/Pt/IrMn-based planar hall sensors with nanoTesla resolution, Sensors and Actuators A 292, 24-29 (2019); https://doi.org/10.1016/j.sna.2019.04.003.
[5] Vijay V. Kondalkar, X. Li, S. Yang, K. Leea. Current Sensor based on Nanocrystalline NiFe/Cu/NiFe, Thin Film, Procedia Eng. 168, 675 - 679 (2016); https://doi:10.1016/j.proeng.2016.11.245.
[6] V. Su Luong, A. Tuan Nguyen, A. Tue Nguyen. Exchange biased spin valve-based gating flux sensor, Measurement 115, 173-177 (2018); https://doi.org/10.1016/j.measurement.2017.10.038.
[7] M.J. Almeidaa, T. Götzea, O. Ueberschära, P. Matthesc, M. Müllerd, R. Eckea, H. Exnerd, S.E. Schulz. Monolithic integration of 2D spin valve magnetic field sensors for angular sensing, Mater. Today: Proceedings 2, 4206-4211 (2015); https://doi.org/10.1016/j.matpr.2015.09.004.
[8] A.A. Kamashev, P.V. Leksin, N.N. Garif'yanov. Superconducting spin-valve effect in a heterostructure containing the Heusler alloy as a ferromagnetic layer, J. Magn. Magn. Mater. 459, 7-11 (2018); https://doi.org/10.1016/j.jmmm.2018.01.085.
[9] C.J. Durrant, L.R. Shelford, R.A.J. Valkass. Dependence of spin pumping and spin transfer torque upon $Ni_{81}Fe_{19}$ thickness in Ta/Ag/$Ni_{81}Fe_{19}$/Ag/Co_2MnGe/Ag/Ta spin-valve structures, Phys. Rev. B 96, 144421 (2017); https://doi.org/10.1103/PhysRevB.96.144421.
[10] T.S. Ramulu, R. Venu, B. Sinha. Synthesis and cysteamine functionalization of CoFe/Au/CoFe nanowires, Thin Solid Films 546, 255-258 (2013); https://doi.org/10.1016/j.tsf.2013.04.080.
[11] R. Matsumoto, H. Arai, S. Yuasa. Spin-transfer-torque switching in a spin-valve nanopillar with a conically magnetized free layer, Appl. Phys. Express. 8, 063007–1–4 (2015). https://doi.org/10.7567/APEX.8.063007.
[12] G.W. Anderson, Y. Huai, M. Pakala. Spin-valve thermal stability: The effect of different antiferromagnets, J. Appl. Phys. 8, 5726-5728 (2000); https://doi.org/10.1063/1.372502.
[13] B. Kocaman, N. Akdoğan. Reduction of shunt current in buffer-free IrMn based spin-valve structures, J. Magn. Magn. Mater. 456, 17-22 (2018); https://doi.org/10.1063/1.372502.
[14] P. Wiśniowski, T. Stobiecki, J. Kanak. Influence of buffer layer texture on magnetic and electrical properties of IrMn spin valve magnetic tunnel junctions, Journal of Applied Physics 100, 013906–1–8 (2006); https://doi.org/10.1063/1.2209180.
[15] P.H. Chan, X. Li, P.W.T. Pong. Spin valves with conetic based synthetic ferrimagnet free layer, Vacuum 140, 111-112 (2017); https://doi.org/10.1016/j.vacuum.2016.09.010.
[16] A.G. Kolesnikov, V.S. Plotnikov, E.V. Pustovalov. Composite topological structure of domain walls in synthetic antiferromagnets, Sci. Report. 8, 15794–1–9 (2018); https://doi.org/10.1038/s41598-018-33780-6.
[17] X.L. Tang, H. Su, H.W. Zhang. Ultra-low-pressure sputtering to improve exchange bias and tune linear ranges in spin valves, J. Magn. Mag.Mater., 429, 65-68 (2017). http://dx.doi.org/10.1016%2Fj.jmmm.2017.01.021.
[18] I.M. Pazukha, I.E. Protsenko. Fe/Cr and Cu/Cr film pressure-sensitive element, Tech. Phys. 55, 571-575 (2010); https://doi.org/10.1134/S1063784210040249.
[19] D. Samal, D. Venkateswarlu, P.S. Anil Kumar. Influence of finite size effect on magnetic and magnetotransport properties of $La_{0.5}Sr_{0.5}CoO_3$ thin films, Solid State Commun. 150 (13–14), 576-580 (2010); https://doi.org/10.1016/j.ssc.2010.01.003
[20] S.I. Protsenko, L.V. Odnodvorets, I.Yu. Protsenko, Nanocomposites, Nanophotonics, Nanobiotechnology, and Applications, ed. By O. Fesenko, L. Yatsenko (Springer, Switzerland, 2015), p.156, https://doi.org/10.1007/978-3-319-06611-0_28.
[21] I.M. Pazukha, Y.O. Shkurdoda, A.M. Chornous, L.V. Dekhtyaruk. Magnetic and magnetoresistive properties of nanocomposites based on Co and SiO, International Journal of Modern Physics B 33 (12), 1950113 (2019); https://doi.org/10.1142/S0217979219501133.
[22] Yu.O. Shkurdoda, V.B. Loboda, L.V. Dekhtyaruk. Specific conductivity of three-layer polycrystalline films, Metallofizika i Noveishie Tekhnologii 30, 295 (2008); https://www.scopus.com/record/display.uri?eid=2-s2.0-49649087930&origin=resultslist.

[23] L. Moraga, R. Henriquez, B. Solis. Quantum theory of the effect of grain boundaries on the electrical conductivity of thin films and wires, Phys. B. 39, 470-471 (2015); http://dx.doi.org/10.1016/j.physb.2015.04.034.
[24] O.V. Pylypenko, I.M. Pazukha., A.S. Ovrutskyi, L.V. Odnodvorets. Electrophysical and Magnetoresistive Properties of Thin Film Alloy $Ni_{80}Fe_{20}$, Journal of Nano- and Electronic Physics 8, 03022 (2016); https://doi.org/10.21272/jnep.8(3).03022.
[25] I.V. Cheshko, A.M. Lohvynov, A.I. Saltykova, S.I. Protsenko. The Structural-Phase State and Diffusion Process in Film Structures Based on Co and Ru, Journal of Nano- and Electronic Physics 10, 06016 (2018); https://doi.org/10.21272/jnep.10(6).06016.
[26] A.M. Lohvynov, M.V. Kostenko, I.V. Cheshko, S.I. Protsenko. Structural-phase state and electrophysical properties of Ru thin films, 2016 International Conference on Nanomaterials: Application & Properties (NAP) 01NTF22 (2016); https://doi.org/10.1109/NAP.2016.7757255.
[27] I.Yu. Protsenko, L.V. Odnodvorets, A.M. Chornous. Electroconductivity and tensosensibility of multilayer films, Metallofizika i Noveishie Tekhnologii 20(1), 36-43 (1998); https://www.scopus.com/record/display.uri?eid=2-s2.0-0342476101&origin=resultslist&sort=cp-f.

А.М. Логвинов, І.В. Чешко, І.М. Пазуха, К.В. Тищенко, О.В. Пилипенко, А.Ю. Загорулько

Вплив товщини проміжного шару Ru на електрофізичні властивості тришарової плівкової системи Co/Ru/Co

Сумський державний університет, Суми, Україна, a.logvinov@aph.sumdu.edu.ua

У даній роботі були проведені дослідження структурно-фазового стану та електрофізичних властивостей тришарових плівкових систем Co/Ru/Co/Sub при зміні товщини шару Ru, d_{Ru} = 5-20 нм. Було показано, що як у свіжо сконденсованому стані, так і після відпалювання до 800 К, фазовий стан системи відповідає ГЩП-Co + ГЩП-Ru. Були отримані залежності питомого опору та температурного коефіцієнту опору як функції d_{Ru}. Показано, що зміна величини питомого опору на першому циклі термообробки стає тим більш сильною, чим більше товщина шару Ru. Величина температурного коефіцієнту опору має порядок 10^{-4} та збільшується з $5{,}05\cdot10^{-4}$ до $6{,}42\cdot10^{-4}$ K^{-1} при зміні товщини d_{Ru} в діапазоні 0-20 нм.

Ключові слова: тришарова плівкова система, пошарова конденсація, електрофізичні властивості, питомий опір, термічний коефіцієнт опору.